

Field theory and structure-preserving geometric particle-in-cell algorithm for drift wave instability and turbulence

Jianyuan Xiao¹ and Hong Qin^{2,1,*}

¹*School of Physical Sciences, University of Science and Technology of China, Hefei, 230026, China*

²*Plasma Physics Laboratory, Princeton University, Princeton, NJ 08543, U.S.A*

Abstract

A field theory and the associated structure-preserving geometric Particle-In-Cell (PIC) algorithm are developed to study low frequency electrostatic perturbations with fully kinetic ions and adiabatic electrons in magnetized plasmas. The algorithm is constructed by geometrically discretizing the field theory using discrete exterior calculus, high-order Whitney interpolation forms, and non-canonical Hamiltonian splitting method. The discretization preserves the non-canonical symplectic structure of the particle-field system, as well as the electromagnetic gauge symmetry. As a result, the algorithm is charge-conserving and possesses long-term conservation properties. Because drift wave turbulence and anomalous transport intrinsically involve multi time-scales, simulation studies using fully kinetic particle demand algorithms with long-term accuracy and fidelity. The structure-preserving geometric PIC algorithm developed adequately servers this purpose. The algorithm has been implemented in the *SymPIC* code, tested and benchmarked using the examples of ion Bernstein waves and drift waves. We apply the algorithm to study the Ion Temperature Gradient (ITG) instability and turbulence in a 2D slab geometry. Simulation results show that at the early stage of the turbulence, the energy diffusion is between the Bohm scaling and gyro-Bohm scaling. At later time, the observed diffusion is closer to the gyro-Bohm scaling, and density blobs generated by the rupture of unstable modes are the prominent structures of the fully developed ITG turbulence.

* hongqin@princeton.edu

1. INTRODUCTION

Drift wave turbulence and associated anomalous transport [1–4] are important physical processes in magnetic fusion devices. They have been intensively studied using the Particle-In-Cell (PIC) methods [5–7], which numerically solve the Vlasov-Maxwell or Vlasov-Poisson equations. The dynamics of charged particles in a magnetic field described by the Vlasov equation contains multiple timescales, e.g., the cyclotron frequencies of electrons and ions, plasma frequency, and the drift wave frequency. When simulating low frequency phenomena directly using the PIC method, the time-step must be chosen small enough to resolve the high frequency dynamics of charged particles. Thus, the total number of time-steps required is large, often exceeding computer resource available. The low frequency drift wave instability is such a case, where the ratio between wave frequency and the electron gyro-frequency is in the order of 10^{-5} . To overcome this difficulty, simplified models which eliminate some of the high-frequency processes while properly describing the slow ion dynamics are developed. A commonly adopted such kinetic model is based on adiabatic electron assumption and quasi-neutrality condition. In this model, for plasmas with one ion species, the ion density n_i , electrons density n_e , and the electrostatic potential ϕ are linked as

$$-\frac{q_i}{q_e}n_i = n_e = n_{e0} \exp\left(-\frac{q_e\phi}{T_e}\right), \quad (1)$$

where q_i and q_e are the charges of ions and electrons, and T_e is the electron temperature. The ion dynamics is governed by Newton's equation with the Lorentz force,

$$\ddot{\mathbf{x}}_p = \frac{q_i}{m_i} [\mathbf{E}(\mathbf{x}_p, t) + \dot{\mathbf{x}}_p \times \mathbf{B}_0(\mathbf{x}_p, t)]. \quad (2)$$

where \mathbf{B}_0 is the background magnetic field, $\mathbf{E} = -\nabla\phi + \mathbf{E}_0$ is the electric field, and \mathbf{E}_0 is the background electric field.

To further decrease computational complexity, gyrokinetic particle simulation methods have been developed and applied to study low frequency instabilities and turbulent transport [8–15]. In spite of the success of gyrokinetic simulations, it was pointed out recently that the basic ordering of the gyrokinetic theory [16–28] is not always valid in certain parameter regimes for modern magnetic fusion devices, especially for the H-mode pedestal physics [29, 30] and when density perturbations are large [31]. Moreover, due to the requirement of accuracy and numerical stability, the time-step Δt in gyrokinetic simulations

are often restricted to the same order of ion gyro-period [32, 33] already. In these situations, the gyrokinetic method has no significant computational advantage over fully kinetic methods. Recently, a fully kinetic ion scheme was developed [34–36]. However, even though adiabatic electron model removes the fast electron dynamics from the system, drift wave instabilities and turbulence still evolve in a slow timescale, about one thousandth of ion gyro-period. Simulating these low frequency physics using fully kinetic ions requires a large number of time-steps, and the long-term conservative properties of the numerical schemes become crucial. Conventional PIC methods are based on direct discretization of differential equations, for which numerical errors in general accumulate coherently during the iterations, and long-term simulation results are not reliable.

In the present study, we use a very different approach to construct an explicit high-order structure-preserving geometric PIC algorithm for simulating low frequency drift wave instabilities and turbulence in magnetized plasmas. First, a field theory for low frequency electrostatic dynamics is established with fully kinetic ions and adiabatic electrons. Then the field theory is geometrically discretized using Discrete Exterior Calculus (DEC) [37, 38], Whitney interpolating forms [39–42], and the powerful Hamiltonian splitting method for Vlasov-Maxwell systems [42–44]. The resulting structure-preserving geometric PIC algorithm is able to preserve the non-canonical symplectic structure associated with the particle-field system, and numerical results show that the simulation error on the energy of the system is bounded by a small number for all time-steps. In addition, the algorithm is gauge independent and thus exactly complies with the discrete local charge conservation law. The knowledge of magnetic potentials is not needed, which is convenient in practical. Furthermore, the algorithm is locally explicit such that it is more efficient on parallel clusters compared with implicit schemes.

In the last ten years, structure-preserving geometric algorithm has become an active research topic in plasma physics. Since 1980s, symplectic integrators for solving Hamiltonian systems have been systematically studied [45–60]. The idea of geometric integrators is to find a discrete one-step iteration map that preserves the symplectic 2-form exactly as the analytical solution of the Hamiltonian system does. According to theoretical and numerical investigations, numerical errors of symplectic integrators on invariants of the systems, such as the total energy and momentum, can be bounded by small numbers for all time-steps [47, 55, 56, 60]. In plasma physics, many fundamental models are canonical or non-canonical

Hamiltonian systems, and corresponding structure-preserving geometric integrators were recently developed, including those for guiding centers [61–68], charged particles [44, 69–79], Vlasov-Maxwell systems [40–42, 80–90], ideal two-fluid systems [91], magnetohydrodynamics [77, 92–94], Schrödinger-Maxwell system [95] and Klein-Gorden-Maxwell [96–98] system. One of the defining characteristics of structure-preserving geometric algorithms is that they are all based on the underpinning field theories and the geometric discretization thereof. Structure-preserving geometric algorithms have demonstrated unparalleled long-term stability and conservative properties compared with conventional non-geometric methods.

The study reported here represents a new development in this research field. We customarily design a field theory for low frequency electrostatic perturbations with fully kinetic ions and adiabatic electrons, and geometrically discrete the field theory to build a structure-preserving geometric PIC algorithm for simulating drift wave instabilities and turbulence in magnetized plasmas.

The paper is organized as follows. In Sec. 2, the field theory for low frequency electrostatic perturbations with fully kinetic ions and adiabatic electrons is established, which is the starting point of our study. Section 3 constructs structure-preserving geometric PIC algorithm by geometrically discretizing the field theory. The algorithm is tested using the examples of Ion Bernstein Waves (IBWs) and drift waves in Sec. 4, and then applied to study the Ion Temperature Gradient (ITG) instability and turbulence in a 2D slab geometry.

2. FIELD THEORY FOR LOW FREQUENCY ELECTROSTATIC PERTURBATIONS

To build an effective geometric PIC algorithm for drift wave instabilities and turbulence, a field theory for low frequency electrostatic perturbations is required. With the assumptions of adiabatic electrons and quasi-neutrality condition, the key of establishing the field theory is to find an appropriate action integral whose Euler-Lagrange (EL) equations recover Eqs. (1) and (2). We have found such an action integral. It is

$$S[\mathbf{x}_p, \phi] = \int dt \left[\sum_p \left(\frac{1}{2} m_i |\dot{\mathbf{x}}_p|^2 + q_i \dot{\mathbf{x}}_p \cdot \mathbf{A}_0(\mathbf{x}_p, t) - q_i \phi(\mathbf{x}_p, t) \right) - \int d\mathbf{x} n_{e0} T_e \exp\left(-\frac{q_e \phi}{T_e}\right) \right], \quad (3)$$

where T_e and n_{e0} are functions of \mathbf{x} and t , \mathbf{A}_0 is the external magnetic potential which gives $\mathbf{B}_0 = \nabla \times \mathbf{A}_0$ and $\mathbf{E}_0 = -\dot{\mathbf{A}}_0$. The system evolves according to the EL equations,

$$\frac{\delta S}{\delta \mathbf{x}_p} = 0 , \quad (4)$$

$$\frac{\delta S}{\delta \phi} = 0. \quad (5)$$

It can be easily verified that Eqs. (4) and (5) are equivalent to Eqs. (2) and (1).

If we insert ϕ obtained from Eq. (5) to the action integral Eq. (3), then the resulting new action integral is

$$S'[\mathbf{x}_p] = \int dt \left[\sum_p \left(\frac{1}{2} m_i |\dot{\mathbf{x}}_p|^2 + q_i \dot{\mathbf{x}}_p \cdot \mathbf{A}_0(\mathbf{x}_p, t) \right) - \int dx^3 (\rho \phi(\rho) - T_e n_{e0} \rho) \right], \quad (6)$$

where

$$\rho(\mathbf{x}) = \sum_p q_i \delta(\mathbf{x} - \mathbf{x}_p) , \quad (7)$$

$$\phi(\rho) = -\frac{T_e}{q_e} \log \left(-\frac{\rho}{n_{e,0} q_e} \right) . \quad (8)$$

The action integral S' does not depend on ϕ , and the corresponding EL equation,

$$\frac{\delta S'}{\delta \mathbf{x}_p} = 0 , \quad (9)$$

is equivalent to Eqs. (4) and (2).

By design, the field theory is only applicable to low frequency electrostatic perturbations with adiabatic electrons. However, it captures the fully kinetic dynamics of ions, and the corresponding geometric algorithm constructed in the next section possesses long-term accuracy and fidelity, a necessity for fully kinetic particle simulations guaranteed only by the structure-preserving nature of the algorithm.

3. STRUCTURE-PRESERVING GEOMETRIC PIC ALGORITHM

In previous study, we have built explicit geometric algorithms for the Vlasov-Maxwell system and ideal two-fluid system [42, 89, 91]. The action integral given by Eq. (3) or (6) is similar to those in previous work. We therefore apply the same techniques of DEC [37, 38] and high-order Whitney interpolating forms [42, 91] to perform the spatial discretization. The resulting spatially discretized action integral is

$$S_{sd}[\mathbf{x}_p, \phi_I] = \int dt L_{sd}[\mathbf{x}_p, \phi_I] , \quad (10)$$

where

$$L_{sd}[\mathbf{x}_p, \phi_I] = \sum_p \left[\frac{1}{2} m_i |\dot{\mathbf{x}}_p|^2 + q_i \dot{\mathbf{x}}_p \cdot \mathbf{A}_0(\mathbf{x}_p, t) - q_i \sum_I W_{\sigma_0 I}(\mathbf{x}_p) \phi_I \right] - \sum_I n_{e0, I} T_{e, I} \exp\left(-\frac{q_e \phi_I}{T_{e, I}}\right) \quad (11)$$

is the spatially discretized Lagrangian. Here, the subscript I is the grid index, $T_{e, I}$ and $n_{e0, I}$ are electron temperature and density fields on the grid, $W_{\sigma_0 I}(\mathbf{x})$ is the Whitney interpolating map for 0-forms (scalar fields) [42, 91]. The equations of motion for the discrete system are

$$\frac{\delta S_{sd}}{\delta \mathbf{x}_p} = 0, \quad (12)$$

$$\frac{\delta S_{sd}}{\delta \phi_I} = 0. \quad (13)$$

Equation (13) plays the role of Poisson's equation, which links the charge density and the electrostatic potential, i.e.,

$$\phi_I = -\frac{T_{e, I}}{q_e} \log\left(-\frac{\rho_I}{n_{e0, I} q_e}\right), \quad (14)$$

$$\rho_I = \sum_p q_i W_{\sigma_0 I}(\mathbf{x}_p). \quad (15)$$

Equation (12) is Newton's equation with the Lorentz force for the p -th particle,

$$\ddot{\mathbf{x}}_p = \frac{q_i}{m_i} \left[\mathbf{E}_0(\mathbf{x}_p, t) + \dot{\mathbf{x}}_p \times \mathbf{B}_0(\mathbf{x}_p, t) - \nabla \sum_I W_{\sigma_0 I}(\mathbf{x}_p) \phi_I \right], \quad (16)$$

where

$$\mathbf{E}_0 = -\dot{\mathbf{A}}_0, \quad (17)$$

$$\mathbf{B}_0 = \nabla \times \mathbf{A}_0. \quad (18)$$

Using the property of Whitney interpolating map [83], Eq. (16) can be rewritten as

$$\ddot{\mathbf{x}}_p = \frac{q_i}{m_i} \left(\mathbf{E}_0(\mathbf{x}_p, t) + \dot{\mathbf{x}}_p \times \mathbf{B}_0(\mathbf{x}_p, t) + \sum_J W_{\sigma_1 J}(\mathbf{x}_p) \mathbf{E}_J \right), \quad (19)$$

where

$$\mathbf{E}_J = -\sum_I \nabla_{d, J, I} \phi_I. \quad (20)$$

Akin to the relationship between $S[\mathbf{x}_p, \phi]$ and $S'[\mathbf{x}_p]$, we can obtain a discrete Lagrangian independent of ϕ_I by inserting Eq. (14) into Eq. (11),

$$L'_{sd}[\mathbf{x}_p] = \sum_p \left[\frac{1}{2} m_i |\dot{\mathbf{x}}_p|^2 + q_i \dot{\mathbf{x}}_p \cdot \mathbf{A}_0(\mathbf{x}_p, t) \right] - V, \quad (21)$$

$$V = \sum_I [\rho_I \phi_I(\rho_I) - T_{e,I} n_{e0,I} \rho_I], \quad (22)$$

$$\rho_I = \sum_p q_i W_{\sigma_0 I}(\mathbf{x}_p). \quad (23)$$

From Eq. (21) we see that the system now involves only particles. It is not difficult to build symplectic algorithms for $L'_{sd}[\mathbf{x}_p]$ using the techniques of variational integrators [59, 60]. However, directly applying these techniques will break the electromagnetic gauge symmetry of the system, which causes charge accumulation and results in numerical stability. To overcome this shortcoming, explicit Hamiltonian splitting method [42–44, 77] for charged particle dynamics and the Vlasov-Maxwell system have been developed. To solve for $L'_{sd}[\mathbf{x}_p]$, here we adopt a similar but more general Hamiltonian splitting method [78].

First, we introduce a non-canonical Hamiltonian structure for the p -th charged particle by extending the phase space into 8-dimensional,

$$H_p(\mathbf{x}_p, \mathbf{v}_p, W_p, t_p) = \frac{1}{2} m_i \mathbf{v}_p^2 - W_p. \quad (24)$$

The associated Poisson bracket is

$$\{F, G\}_p = \nabla_p F \begin{bmatrix} 0 & \frac{1}{m_i} I & 0 & 0 \\ -\frac{1}{m_i} I & \frac{q_i}{m_i^2} \hat{B}_0(\mathbf{x}_p, t_p) & \left(\frac{q_i}{m_i} \frac{\partial \mathbf{A}_0(\mathbf{x}_p, t_p)}{\partial t_p} \right)^T & 0 \\ 0 & -\frac{q_i}{m_i} \frac{\partial \mathbf{A}_0(\mathbf{x}_p, t_p)}{\partial t_p} & 0 & -1 \\ 0 & 0 & 1 & 0 \end{bmatrix} (\nabla_p G)^T, \quad (25)$$

where

$$\nabla_p F = \left[\frac{\partial F}{\partial \mathbf{x}_p}, \frac{\partial F}{\partial \mathbf{v}_p}, \frac{\partial F}{\partial W_p}, \frac{\partial F}{\partial t_p} \right], \quad (26)$$

$$\hat{B}_0 = \begin{bmatrix} 0 & B_{0,z} & -B_{0,y} \\ -B_{0,z} & 0 & B_{0,x} \\ B_{0,y} & -B_{0,x} & 0 \end{bmatrix}. \quad (27)$$

The Hamiltonian H and Poisson bracket $\{\cdot, \cdot\}$ for the extended system are

$$H = \sum_p H_p + V, \\ \{F, G\} = \sum_p \{F, G\}_p,$$

where V is defined in Eq. (22). Hamilton's equation is

$$\dot{f} = \{f, H\} \text{ , for } f \in \{\mathbf{x}_p, \mathbf{v}_p, W_p, t_p\} \text{ .} \quad (28)$$

Newton's equation with the Lorentz force (16) is equivalent to $\dot{\mathbf{v}}_p = \{\mathbf{v}_p, H\}$ and $\dot{\mathbf{x}}_p = \{\mathbf{x}_p, H\}$.

Next, we split the Hamiltonian H into 5 parts,

$$H = H_x + H_y + H_z + H_W + H_V \text{ ,} \quad (29)$$

where $H_W = -\sum_p W_p$, $H_V = V$, $H_x = \sum_p m_i v_{p,x}^2/2$, $H_y = \sum_p m_i v_{p,y}^2/2$, and $H_z = \sum_p m_i v_{p,z}^2/2$. Each part represents a sub-Hamiltonian system. For example, the equation of motion generated by H_V is

$$\dot{f} = \{f, H_V\} \text{ ,} \quad (30)$$

i.e.,

$$\left\{ \begin{array}{l} \dot{\mathbf{x}}_p = 0 \text{ ,} \\ \dot{\mathbf{v}}_p = \partial V / \partial \mathbf{x}_p \text{ ,} \\ \dot{W}_p = 0 \text{ ,} \\ \dot{t}_p = 0 \text{ ,} \end{array} \right. \quad \text{for all } p \text{ .} \quad (31)$$

Its exact solution map $\Theta_V(\Delta t)$ is

$$\Theta_V(\Delta t) : \left\{ \begin{array}{l} \mathbf{x}_p \rightarrow \mathbf{x}_p \text{ ,} \\ \mathbf{v}_p \rightarrow \mathbf{v}_p + \Delta t \partial V / \partial \mathbf{x}_p \text{ ,} \\ W_p \rightarrow W_p \text{ ,} \\ t_p \rightarrow t_p \text{ ,} \end{array} \right. \quad \text{for all } p \text{ .} \quad (32)$$

We can exactly solve all other sub-systems H_W , H_x , H_y and H_z in a similar way. The exact

solution maps are listed as follows.

For all p : (33)

$$\Theta_W(\Delta t) : \begin{cases} \mathbf{x}_p \rightarrow \mathbf{x}_p , \\ \mathbf{v}_p \rightarrow \mathbf{v}_p - \frac{q_i}{m_i} (\mathbf{A}_0(\mathbf{x}_p, t_p + \Delta t) - \mathbf{A}_0(\mathbf{x}_p, t_p)) , \\ W_p \rightarrow W_p , \\ t_p \rightarrow t_p + \Delta t . \end{cases} \quad (34)$$

$$\Theta_x(\Delta t) : \begin{cases} \mathbf{x}_p \rightarrow \mathbf{x}_{sp} + \Delta t v_{x,p} \mathbf{e}_x , \\ \mathbf{v}_p \rightarrow \mathbf{v}_p + \frac{q_i}{m_i} v_{x,p} \mathbf{e}_x \times \int_0^{\Delta t} dt' \mathbf{B}_0(\mathbf{x}_p + v_{x,p} t' \mathbf{e}_x, t_p) , \\ W_p \rightarrow W_p - \Delta t \frac{q_i}{m_i} \int_0^{\Delta t} dt' \frac{\partial \mathbf{A}_0(\mathbf{x}_p + v_{x,p} t' \mathbf{e}_x, t_p)}{\partial t_p} , \\ t_p \rightarrow t_p . \end{cases} \quad (35)$$

$$\Theta_y(\Delta t) : \begin{cases} \mathbf{x}_p \rightarrow \mathbf{x}_{sp} + \Delta t v_{y,p} \mathbf{e}_y , \\ \mathbf{v}_p \rightarrow \mathbf{v}_p + \frac{q_i}{m_i} v_{y,p} \mathbf{e}_y \times \int_0^{\Delta t} dt' \mathbf{B}_0(\mathbf{x}_p + v_{y,p} t' \mathbf{e}_y, t_p) , \\ W_p \rightarrow W_p - \Delta t \frac{q_i}{m_i} \int_0^{\Delta t} dt' \frac{\partial \mathbf{A}_0(\mathbf{x}_p + v_{y,p} t' \mathbf{e}_y, t_p)}{\partial t_p} , \\ t_p \rightarrow t_p . \end{cases} \quad (36)$$

$$\Theta_z(\Delta t) : \begin{cases} \mathbf{x}_p \rightarrow \mathbf{x}_{sp} + \Delta t v_{z,p} \mathbf{e}_z , \\ \mathbf{v}_p \rightarrow \mathbf{v}_p + \frac{q_i}{m_i} v_{z,p} \mathbf{e}_z \times \int_0^{\Delta t} dt' \mathbf{B}_0(\mathbf{x}_p + v_{z,p} t' \mathbf{e}_z, t_p) , \\ W_p \rightarrow W_p - \Delta t \frac{q_i}{m_i} \int_0^{\Delta t} dt' \frac{\partial \mathbf{A}_0(\mathbf{x}_p + v_{z,p} t' \mathbf{e}_z, t_p)}{\partial t_p} , \\ t_p \rightarrow t_p . \end{cases} \quad (37)$$

Using these exact solutions of the subsystems, we can compose symplectic iteration schemes of the entire system. For instance, a 1st-order symplectic scheme is

$$\Theta_1(\Delta t) = \Theta_x(\Delta t) \Theta_y(\Delta t) \Theta_z(\Delta t) \Theta_V(\Delta t) \Theta_W(\Delta t) , \quad (38)$$

and a symmetric 2nd-order symplectic scheme can be built as

$$\begin{aligned} \Theta_2(\Delta t) &= \Theta_W(\Delta t/2) \Theta_x(\Delta t/2) \Theta_y(\Delta t/2) \Theta_z(\Delta t/2) \Theta_V(\Delta t) \\ &\quad \Theta_z(\Delta t/2) \Theta_y(\Delta t/2) \Theta_x(\Delta t/2) \Theta_W(\Delta t/2) . \end{aligned} \quad (39)$$

A $2(l+1)$ -th order symplectic scheme can be constructed from a $2l$ -th order symplectic scheme as [99]

$$\Theta_{2(l+1)}(\Delta t) = \Theta_{2l}(\alpha_l \Delta t) \Theta_{2l}(\beta_l \Delta t) \Theta_{2l}(\alpha_l \Delta t) , \quad (40)$$

$$\alpha_l = 1/(2 - 2^{1/(2l+1)}) , \quad (41)$$

$$\beta_l = 1 - 2\alpha_l . \quad (42)$$

We should point out that there exist a discrete variational approach that generates the same explicit schemes as Θ_1 , Θ_2 and Θ_{2l} . See Refs. [78, 89] for details.

4. SIMULATIONS OF ION BERNSTEIN WAVES AND DRIFT WAVE INSTABILITIES

We have implemented the 2nd-order explicit structure-preserving geometric PIC algorithm given by Eq. (39) in the *SympIC* code to simulate low-frequency electrostatic perturbations with fully kinetic ions and adiabatic electrons. The Whitney interpolating maps are chosen to be the same as those in Ref. [91]. As a benchmark and test, the algorithm is applied to study the ion Bernstein waves. It is then used to simulate the drift wave instability and ion temperature gradient turbulence in a 2D slab geometry.

4.1. Dispersion relation of ion Bernstein waves

To simulate the IBWs in a homogeneous magnetized plasma, the follow system parameters are chosen. External magnetic field is in the z -direction, $\mathbf{B}_0 = B_{0,z}\mathbf{e}_z$ with $B_{0,z} = 2.5\text{T}$. Plasma density $n_{i,0} = 1 \times 10^{18}\text{m}^{-3}$, and the thermal velocity of ions $v_{T,i,0} = 7.23 \times 10^{-4}c$, where c is the speed of light in the vacuum. The mass and charge of ions are $m_i = 3.342 \times 10^{-27}\text{kg}$ and $q_i = 1.6 \times 10^{-19}\text{C}$, respectively. The simulation domain is a $256 \times 1 \times 1$ grid and periodic boundaries are imposed for all 3 directions. On average there are 256 simulation particles (sampling points) per grid cell. The grid sizes are $\Delta x = 4 \times 10^{-4}\text{m} = 0.2208\rho_{T,i}$ and $\Delta t = 120\Delta x/c = 0.0192/\omega_{c,i}$. Here the time-step Δt is relatively small compared with the cyclone period $2\pi/\omega_{c,i}$, because it needs to satisfy the Courant condition for stability. Initially the perturbed electromagnetic fields is set to zero, and electrostatic waves are generated from noise. The total number of time-steps is 8192.

Theoretically the dispersion relation of the electrostatic IBWs in the x -direction is [34, 100]

$$\epsilon(\omega, k) = 1 + \frac{\theta}{\rho_{T,i}} \sum_{n=-\infty}^{\infty} n I_n(b) \exp(-b) \frac{v_{T,i,0}}{\omega + n\omega_{c,i}}, \quad (43)$$

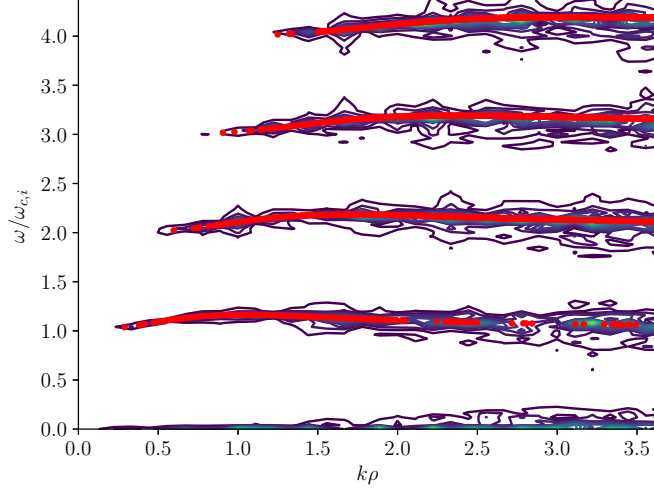


Figure 1. Dispersion relation of ion Bernstein waves in a hot magnetized plasma simulated by structure-preserving geometric PIC algorithm. Red dots are analytical dispersion relation.

where

$$b = k^2 \rho_{T,i}^2, \quad \theta = T_e/T_i = 1, \quad T_i = m_i v_{T,i,0}^2,$$

$$\omega_{c,i} = q_i B_{0,z}/m_i, \quad \rho_{T,i} = m_i v_{T,i,0}/(q_i B_{0,z}).$$

The spectra of the electric field in the x -direction is plotted in Fig. 1, which clearly shows that the simulated dispersion relation matches the theoretical result very well.

To test the energy conservation property, we performed a long-term simulation. The total number of time-steps is 1×10^6 . The simulation domain is a $32 \times 32 \times 32$ grid mesh, and the averaged number of simulation particles per cell is 16. During the simulation the total energy is recorded, and the result is shown in Fig. 2. It is evident that the error of total energy is bounded by a small number for all simulation time-steps.

4.2. Ion temperature gradient instability and turbulence in a slab geometry

In certain parameter regimes, the ion temperature gradient in a magnetized plasma can excite the drift wave instability, which often nonlinearly evolves into a turbulent stage to produce anomalous transport of energy and particles [1–4, 15, 34–36, 101–108]. We demonstrate the simulations of the ITG instability and turbulence by the structure-preserving geometric PIC algorithm in a 2D slab geometry. System parameters are similar to those in

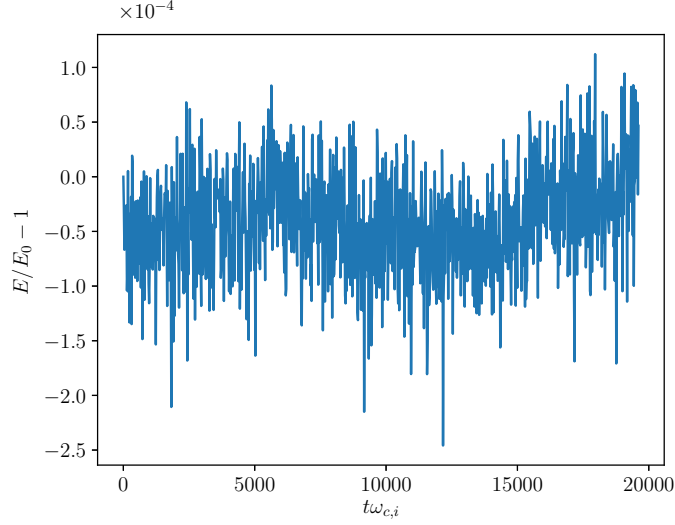


Figure 2. The energy error of structure-preserving geometric PIC algorithm is bounded by a small number for all simulation time-steps.

Sec. 4.4.1, except that the temperatures for both ions and electrons are now functions of the x -coordinate,

$$T_e(x) = T_i(x) = m_i v_{T,i,0}^2 \exp\left(-\frac{(x-x_m)^2}{\sigma^2}\right), \quad (44)$$

$$x_m = 256\Delta x, \quad \sigma = 44.72\Delta x. \quad (45)$$

The simulation domain is a $N_x \times N_y \times N_z = 512 \times 512 \times 1$ grid, and the total number of time-steps is 1.2×10^6 . To balance the pressure gradient for equilibrium, we use an external electric field, which is set to

$$\mathbf{E}_0(x, y, z) = \frac{\partial T_i(x)}{\partial x} \frac{1}{q_i}. \quad (46)$$

It can be checked that the local Maxwell distribution function

$$f_0(\mathbf{x}, \mathbf{v}) = \frac{n_0}{(2\pi T_i(x)/m_i)^{3/2}} \exp\left(-\frac{|\mathbf{v}|^2}{T_i(x)/m_i}\right), \quad (47)$$

is the steady state solution of the 0th, 1st, and 2nd-order moment equations of the Vlasov equation, i.e.,

$$\begin{aligned} \int d^3v \left(\mathbf{v} \cdot \nabla f_0 + \frac{q_i}{m_i} (\mathbf{E}_0 + \mathbf{v} \times \mathbf{B}_0) \frac{\partial}{\partial \mathbf{v}} f_0 \right) &= 0, \\ \int d^3v \left(\mathbf{v}\mathbf{v} \cdot \nabla f_0 + \mathbf{v} \frac{q_i}{m_i} (\mathbf{E}_0 + \mathbf{v} \times \mathbf{B}_0) \frac{\partial}{\partial \mathbf{v}} f_0 \right) &= 0, \\ \int d^3v \left(\mathbf{v}\mathbf{v}\mathbf{v} \cdot \nabla f_0 + \mathbf{v}\mathbf{v} \frac{q_i}{m_i} (\mathbf{E}_0 + \mathbf{v} \times \mathbf{B}_0) \frac{\partial}{\partial \mathbf{v}} f_0 \right) &= 0. \end{aligned}$$

To obtain a more precise kinetic equilibrium, we first use the f_0 specified by Eq.(47) to perform a 1-D simulation, i.e., $N_y = 1$. After 10^6 time-steps when the ion distribution function reaches a steady state, we take this numerically calculated distribution function as the equilibrium distribution function for the 2D simulation in the slab geometry. For the system parameters selected in this example, the ion temperature gradient excites unstable drift modes. According to the theory of drift wave, the phase velocity in the y -direction of modes is approximately

$$v_{d,y}(x) = \frac{\partial T_i(x)}{\partial x} \frac{1}{m_i \omega_{c,i}}. \quad (48)$$

Plotted in Fig. 3 are the phase velocity in the y -direction calculated from the electric field perturbations observed in the simulation and the theoretical drift velocity $v_{d,y}(x)$ as a function of x given by Eq. (48). It is clear that the simulation agrees with the theoretical prediction very well. We also plotted in Fig. 3 the averaged bulk velocity of the ions in the y -direction, which by comparison is smaller. This indicates that the space-time structure observed in the simulation is produced by the drift wave, instead of the bulk flow of the ions.

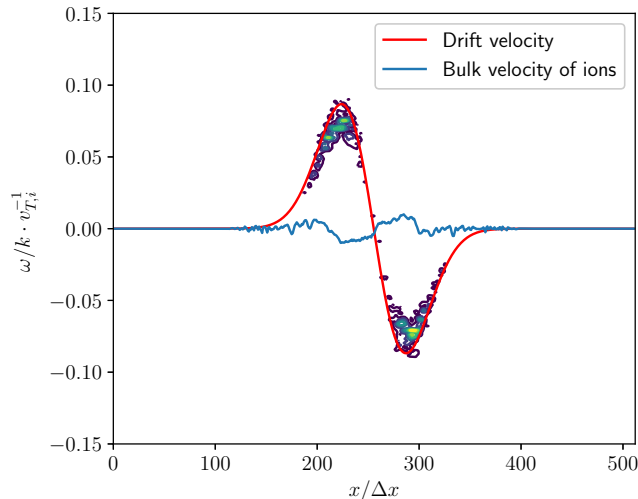


Figure 3. Phase velocity in the y -direction as a function of x at $k_y = 40\pi/(512\Delta x)$ and $t = 766/\omega_{c,i}$. Solid lines are the theoretical value of $v_{d,y}(x)$ (red) given by Eq. (48) and the bulk velocity of the ions in the y -direction (blue).

To illustrate the instability, the time history of the amplitude of density perturbation with different k_y at $x = 224\Delta x$ are plotted in Fig. 4. We observe that all modes displayed

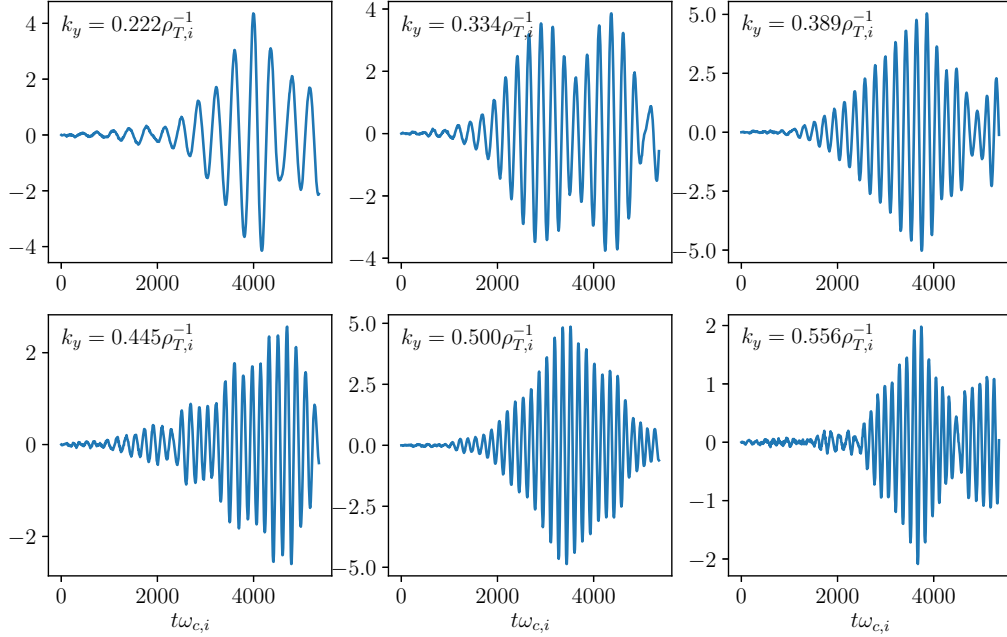


Figure 4. Time history of the amplitude of the unstable modes at $x = 224\Delta x$ for different values of k_y .

grow initially, and saturate after $t > 3000/\omega_{c,i}$. From the simulation data, the dispersion relation of the instability at $x = 224\Delta x$ can be calculated. It is plotted in Fig. 5.

After a sufficient long time, the unstable modes nonlinearly evolve into a turbulent state, as evident from the distribution of kinetic energy density and number density of ions at different times. Figure 6 shows that the kinetic energy diffuses as the instability grows, saturates, and becomes turbulent. Figure 7 shows that density blobs generated by the rupture of unstable modes are the prominent structures of the fully developed ITG turbulence. The details of the instability and turbulence, especially the formation of density blobs, can be observed from the video of the density evolution available at <http://staff.ustc.edu.cn/~xiao jy/ditg.html>.

When turbulence develops, the energy or particle diffusion of the plasma across the magnetic field is conjectured empirically to follow the scaling of Bohm diffusion or the gyro-

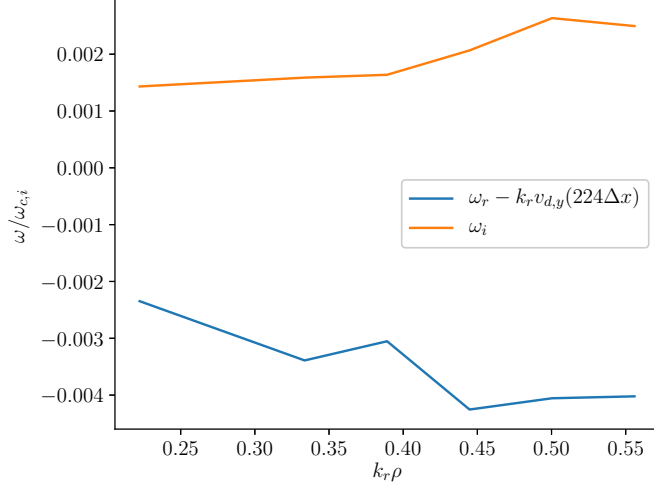


Figure 5. Dispersion relation of unstable modes at $x = 224\Delta x$ calculated from simulation data.

Bohm diffusion [109–112]. The corresponding diffusion coefficients are

$$\chi_B = \frac{k_B T_i}{16q_i B}, \quad (49)$$

$$\chi_{gB} = \rho^* \chi_B, \quad (50)$$

where $\rho^* = \rho_{T,i}/L$ is the gyro-radius of ions measured in L , the characteristic length of the plasma. Assuming that the diffusion coefficient varies slowly with x and the energy density E_k diffuses according to

$$\dot{E}_k = \chi \frac{d^2 E_k}{dx^2}, \quad (51)$$

we can calculate the numerical diffusion coefficient of ions χ in the x -direction. The results are plotted in Fig. 8, where the local plasma characteristic length L is estimated using

$$L = \frac{E_k}{dE_k/dx}. \quad (52)$$

We observe that at $t = 3841/\omega_{c,i}$ the diffusion coefficient χ is between the Bohm scaling χ_B and gyro-Bohm scaling χ_{gB} . Afterwards, χ decreases. When the ITG turbulence is fully developed at $t = 19159/\omega_{c,i}$, the diffusion coefficient χ is closer to the gyro-Bohm scaling χ_{gB} .

We emphasize again that simulating long-term dynamical and transport behavior of magnetized plasmas using fully kinetic particles demands a large number of simulation time-steps, 1.2×10^6 in this case. A structure-preserving geometric algorithm with long-term

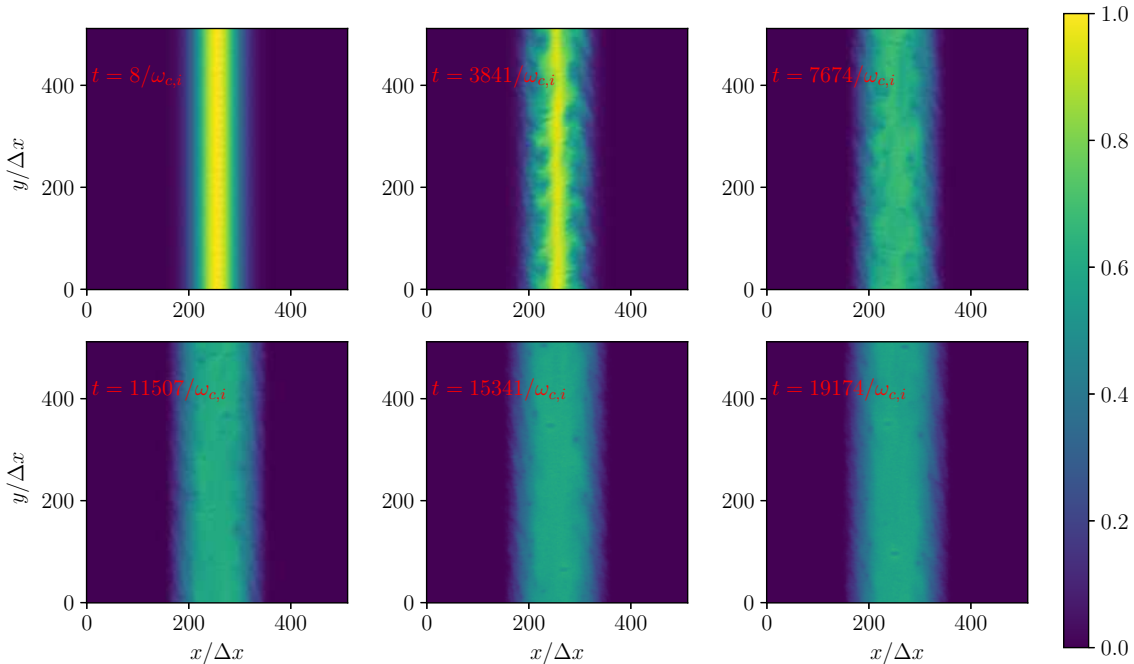


Figure 6. The kinetic energy diffuses as the instability grows, saturates, and becomes turbulent.

accuracy and fidelity is desirable for this purpose. To verify the long-term conservative properties of the simulation, we plotted the energy error in Fig. 9. Clearly, the error is globally bounded by a small number for all simulation time-steps.

5. DISCUSSION AND CONCLUSION

In conclusion, we have customarily designed a field theory for low frequency electrostatic perturbations with fully kinetic ions and adiabatic electrons, and geometrically discretized the field theory to build a structure-preserving geometric PIC algorithm for simulating drift wave instabilities and turbulence in magnetized plasmas. The geometric discretization of the field theory is accomplished using DEC, high-order Whitney interpolation forms, and the non-canonical Hamiltonian splitting method. It preserves the non-canonical symplectic structure of the particle-field system, as well as the gauge symmetry. And as a result, the PIC algorithm is automatically charge-conserving and possesses long-term conservation properties that are indispensable for simulating the dynamics of fully kinetic particles. We have successfully implemented the algorithm in the *SymPIC* code. The algorithm was tested

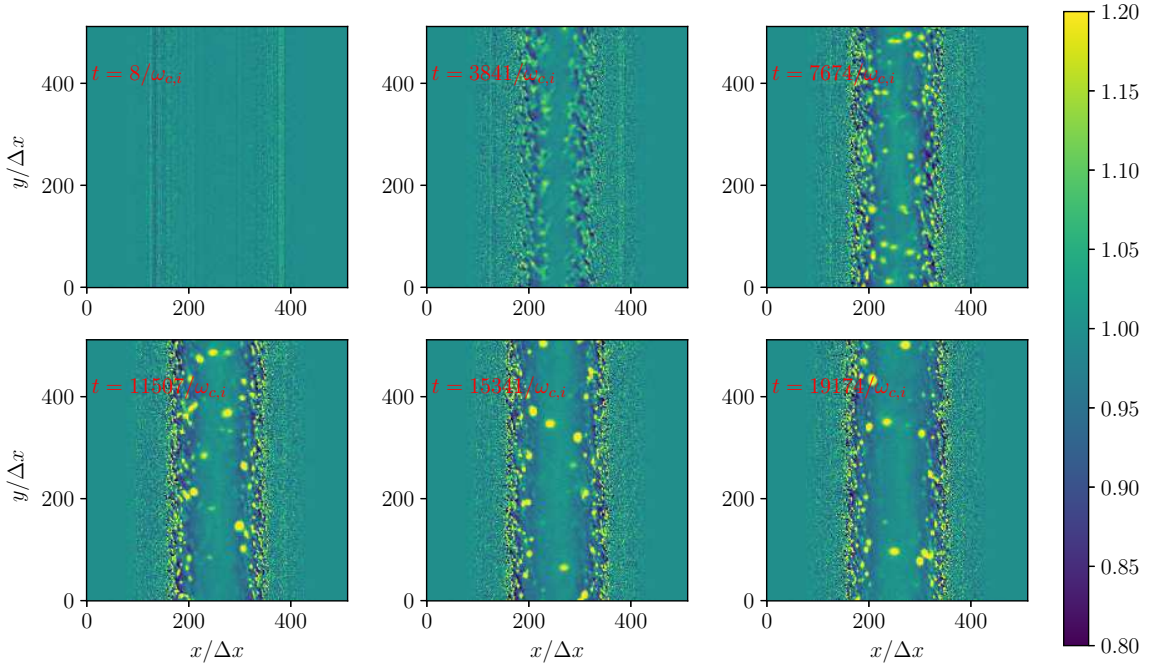


Figure 7. Density perturbation at different times. Density blobs generated by the rupture of unstable modes are the prominent structures of the fully developed ITG turbulence.

and benchmarked using the examples of ion Bernstein waves and drift waves, and applied to study the ion temperature gradient instability and turbulence in a 2D slab geometry. Simulation results show that at the early stage of the ITG turbulence, the energy diffusion is between the Bohm scaling and gyro-Bohm scaling. At later time, the observed diffusion is closer to the gyro-Bohm scaling, and density blobs generated by the rupture of unstable modes are the prominent structures of the fully developed ITG turbulence.

ACKNOWLEDGMENTS

This research was supported by the National Key Research and Development Program (2016YFA0400600, 2016YFA0400601 and 2016YFA0400602), the National Natural Science Foundation of China (NSFC-11775219 and NSFC-11575186), China Postdoctoral Science Foundation (2017LH002), the Fundamental Research Funds for the Central Universities

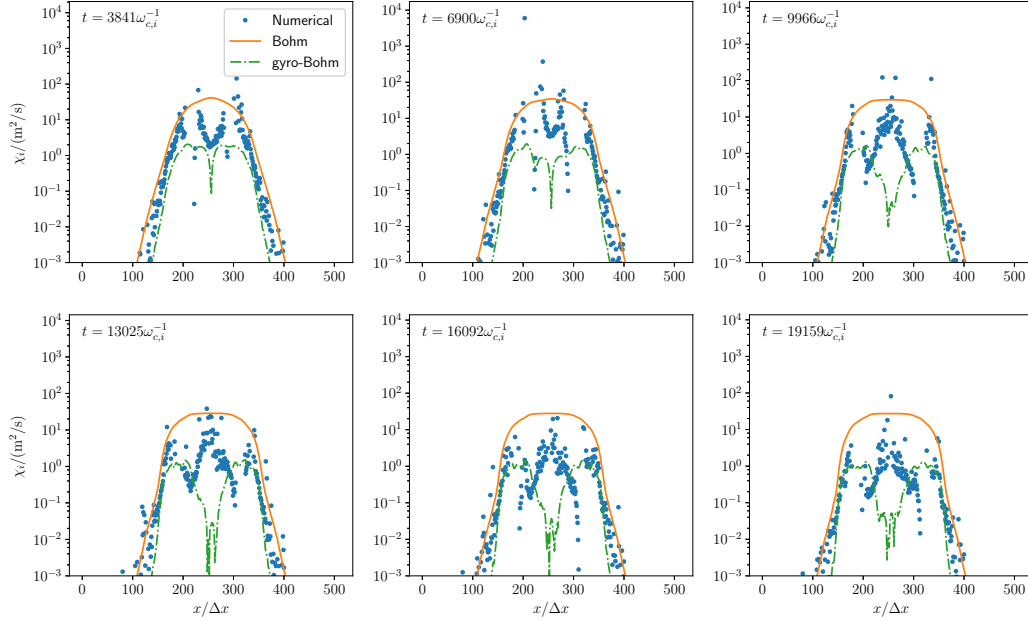


Figure 8. Energy diffusion coefficient in the x -direction at different times. The diffusion coefficient is closer to the gyro-Bohm scaling when the ITG turbulence is fully developed.

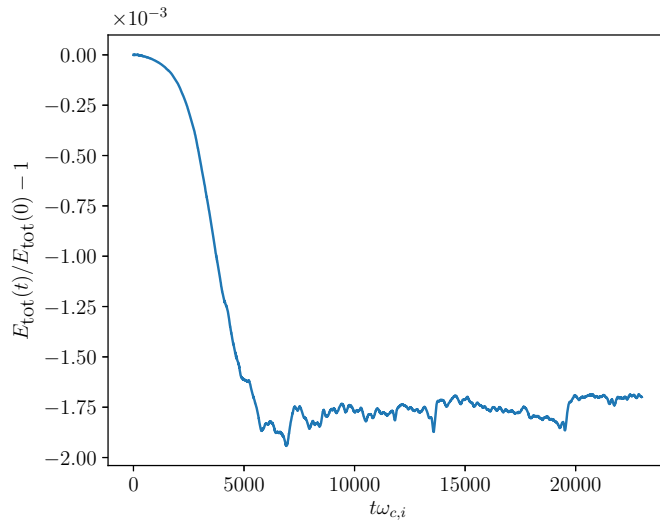


Figure 9. Time history of the energy error of ITG turbulence simulation using the structure-preserving geometric PIC algorithm. The error is globally bounded by a small number for all simulation time-steps.

(WK2030040096) and the U.S. Department of Energy (DE-AC02-09CH11466).

- [1] N. A. Krall and M. N. Rosenbluth, *Physics of Fluids* **8**, 1488 (1965).
- [2] B. Coppi, *Physics of Fluids* **10**, 582 (1967).
- [3] W. Tang, *Nuclear Fusion* **18**, 1089 (1978).
- [4] W. Horton, *Reviews of Modern Physics* **71**, 735 (1999).
- [5] J. M. Dawson, *Reviews of Modern Physics* **55**, 403 (1983).
- [6] R. W. Hockney and J. W. Eastwood, *Computer Simulation Using Particles* (CRC Press, 1988).
- [7] C. K. Birdsall and A. B. Langdon, *Plasma Physics via Computer Simulation* (IOP Publishing, 1991).
- [8] W. W. Lee, *Physics of Fluids* **26**, 556 (1983).
- [9] A. Dimits and W. W. Lee, *Journal of Computational Physics* **107**, 309 (1993).
- [10] S. Parker and W. Lee, *Physics of Fluids B: Plasma Physics* **5**, 77 (1993).
- [11] S. Parker, W. Lee, and R. Santoro, *Physical Review Letters* **71**, 2042 (1993).
- [12] G. Hu and J. A. Krommes, *Physics of Plasmas* **1**, 863 (1994).
- [13] A. Dimits, T. Williams, J. Byers, and B. Cohen, *Physical Review Letters* **77**, 71 (1996).
- [14] Z. Lin, T. S. Hahm, W. Lee, W. M. Tang, and R. B. White, *Science* **281**, 1835 (1998).
- [15] S. E. Parker, C. Kim, and Y. Chen, *Physics of Plasmas* **6**, 1709 (1999).
- [16] E. A. Frieman, R. C. Davidson, and B. Langdon, *Physics of Fluids* **9**, 1475 (1966).
- [17] P. J. Catto, *Plasma Physics and Controlled Fusion* **20**, 719 (1978).
- [18] E. Frieman and L. Chen, *The Physics of Fluids* **25**, 502 (1982).
- [19] D. H. E. Dubin, J. A. Krommes, C. Oberman, and W. W. Lee, *Physics of Fluids* **26**, 3524 (1983).
- [20] T. S. Hahm, *Physics of Fluids* **31**, 2670 (1988).
- [21] A. Brizard, *Journal of Plasma Physics* **41**, 541 (1989).
- [22] H. Qin, W. M. Tang, and G. Rewoldt, *Physics of Plasmas* **5**, 1035 (1998).
- [23] H. Qin, W. M. Tang, and W. W. Lee, *Physics of Plasmas* **7**, 4433 (2000).
- [24] H. Qin and W. M. Tang, *Physics of Plasmas* **11**, 1052 (2004).
- [25] H. Qin, *Fields Institute Communications* **46**, 171 (2005).

- [26] H. Qin, R. Cohen, W. Nevins, and X. Xu, *Physics of Plasmas* **14**, 056110 (2007).
- [27] J. W. Burby, *Chasing Hamiltonian Structure in Gyrokinetic Theory*, Ph.D. thesis, Princeton University (2015).
- [28] J. Burby, A. Brizard, P. Morrison, and H. Qin, *Physics Letters A* **379**, 2073 (2015).
- [29] S. Wan and Y. C. Parker, *Phys. Rev. Lett* **109**, 185004 (2012).
- [30] W. Wan, S. E. Parker, Y. Chen, R. J. Groebner, Z. Yan, A. Y. Pankin, and S. E. Kruger, *Physics of Plasmas* **20**, 055902 (2013).
- [31] Z. Deng and R. Waltz, *Physics of Plasmas* **22**, 056101 (2015).
- [32] Y. Chen, S. E. Parker, G. Rewoldt, S.-H. Ku, G.-Y. Park, and C.-S. Chang, *Physics of Plasmas* **15**, 055905 (2008).
- [33] J. Chowdhury, Y. Chen, W. Wan, S. E. Parker, W. Guttenfelder, and J. Canik, *Physics of Plasmas* **23**, 012513 (2016).
- [34] M. T. Miecniowski, B. J. Sturdevant, Y. Chen, and S. E. Parker, *Physics of Plasmas* **25**, 055901 (2018).
- [35] B. Sturdevant, Y. Chen, and S. Parker, *Physics of Plasmas* **24**, 081207 (2017).
- [36] Y. Hu, M. Miecniowski, Y. Chen, and S. Parker, *Plasma* **1**, 105 (2018).
- [37] A. N. Hirani, *Discrete Exterior Calculus*, Ph.D. thesis, California Institute of Technology (2003).
- [38] M. Desbrun, A. N. Hirani, M. Leok, and J. E. Marsden, <http://arxiv.org/abs/math/0508341v2>.
- [39] H. Whitney, *Geometric Integration Theory* (Princeton University Press, 1957).
- [40] J. Squire, H. Qin, and W. M. Tang, *Geometric Integration of the Vlasov-Maxwell System with a Variational Particle-in-cell Scheme*, Tech. Rep. PPPL-4748 (Princeton Plasma Physics Laboratory, 2012).
- [41] J. Squire, H. Qin, and W. M. Tang, *Physics of Plasmas* **19**, 084501 (2012).
- [42] J. Xiao, H. Qin, J. Liu, Y. He, R. Zhang, and Y. Sun, *Physics of Plasmas* **22**, 112504 (2015).
- [43] Y. He, H. Qin, Y. Sun, J. Xiao, R. Zhang, and J. Liu, *Physics of Plasmas* **22**, 124503 (2015).
- [44] Y. He, Z. Zhou, Y. Sun, J. Liu, and H. Qin, *Physics Letters A* **381**, 568 (2017).
- [45] R. D. Ruth, *IEEE Transactions on Nuclear Science* **30**, 2669 (1983).
- [46] K. Feng, in *the Proceedings of 1984 Beijing Symposium on Differential Geometry and Differential Equations*, edited by K. Feng (Science Press, 1985) pp. 42–58.

- [47] K. Feng, *Journal of Computational Mathematics* **4**, 279 (1986).
- [48] K. Feng and M. Qin, *Symplectic Geometric Algorithms for Hamiltonian Systems* (Springer, 2010).
- [49] E. Forest and R. D. Ruth, *Physica D* **43**, 105 (1990).
- [50] P. J. Channell and C. Scovel, *Nonlinearity* **3**, 231 (1990).
- [51] J. Candy and W. Rozmus, *Journal of Computational Physics* **92**, 230 (1991).
- [52] J. Hong and M. Z. Qin, *Applied Mathematics Letters* **15**, 1005 (2002).
- [53] Y.-F. Tang, *Computers & Mathematics with Applications* **25**, 83 (1993).
- [54] Z. Shang, *Journal of Computational Mathematics* **2**, 265 (1994).
- [55] Z. Shang, *Numerische Mathematik* **83**, 477 (1999).
- [56] J. M. Sanz-Serna and M. P. Calvo, *Numerical Hamiltonian Problems* (Chapman and Hall, London, 1994).
- [57] J. E. Marsden, G. W. Patrick, and S. Shkoller, *Communications in Mathematical Physics* **199**, 351 (1998).
- [58] Y. Sun and M. Qin, *Journal of Mathematical Physics* **41**, 7854 (2000).
- [59] J. E. Marsden and M. West, *Acta Numer.* **10**, 357 (2001).
- [60] E. Hairer, C. Lubich, and G. Wanner, *Geometric Numerical Integration: Structure-preserving Algorithms for Ordinary Differential Equations*, Vol. 31 (Springer, 2006).
- [61] H. Qin and X. Guan, *Physical Review Letters* **100**, 035006 (2008).
- [62] H. Qin, X. Guan, and W. M. Tang, *Physics of Plasmas* **16**, 042510 (2009).
- [63] R. Zhang, J. Liu, Y. Tang, H. Qin, J. Xiao, and B. Zhu, *Physics of Plasmas* **21**, 032504 (2014).
- [64] C. L. Ellison, J. M. Finn, H. Qin, and W. M. Tang, *Plasma Physics and Controlled Fusion* **57**, 054007 (2015).
- [65] J. Burby and C. Ellison, *Physics of Plasmas* **24**, 110703 (2017).
- [66] M. Kraus, <http://arxiv.org/abs/1708.07356v1>.
- [67] C. L. Ellison, J. M. Finn, J. W. Burby, M. Kraus, H. Qin, and W. M. Tang, *Physics of Plasmas* **25**, 052502 (2018).
- [68] C. L. Ellison, *Development of Multistep and Degenerate Variational Integrators for Applications in Plasma Physics*, Ph.D. thesis, Princeton University (2016).

- [69] H. Qin, S. Zhang, J. Xiao, J. Liu, Y. Sun, and W. M. Tang, *Physics of Plasmas* **20**, 084503 (2013).
- [70] Y. He, Y. Sun, J. Liu, and H. Qin, *Journal of Computational Physics* **281**, 135 (2015).
- [71] R. Zhang, J. Liu, H. Qin, Y. Wang, Y. He, and Y. Sun, *Physics of Plasmas* **22**, 044501 (2015).
- [72] C. Ellison, J. Burby, and H. Qin, *Journal of Computational Physics* **301**, 489 (2015).
- [73] R. Zhang, H. Qin, Y. Tang, J. Liu, Y. He, and J. Xiao, *Physical Review E* **94**, 013205 (2016).
- [74] Y. Wang, J. Liu, and H. Qin, *Physics of Plasmas* **23**, 122513 (2016).
- [75] Y. He, Y. Sun, J. Liu, and H. Qin, *Journal of Computational Physics* **305**, 172 (2016).
- [76] X. Tu, B. Zhu, Y. Tang, H. Qin, J. Liu, and R. Zhang, *Physics of Plasmas* **23**, 122514 (2016).
- [77] Z. Zhou, Y. He, Y. Sun, J. Liu, and H. Qin, *Physics of Plasmas* **24**, 052507 (2017).
- [78] J. Xiao and H. Qin, <http://arxiv.org/abs/1809.03697v1>.
- [79] Y. Shi, Y. Sun, Y. He, H. Qin, and J. Liu, *Numerical Algorithms* (2019), 10.1007/s11075-018-0636-6.
- [80] J. Xiao, J. Liu, H. Qin, and Z. Yu, *Physics of Plasmas* **20**, 102517 (2013).
- [81] E. Evstatiev and B. Shadwick, *Journal of Computational Physics* **245**, 376 (2013).
- [82] B. A. Shadwick, A. B. Stamm, and E. G. Evstatiev, *Physics of Plasmas* **21**, 055708 (2014).
- [83] J. Xiao, J. Liu, H. Qin, Z. Yu, and N. Xiang, *Physics of Plasmas* **22**, 092305 (2015).
- [84] H. Qin, J. Liu, J. Xiao, R. Zhang, Y. He, Y. Wang, Y. Sun, J. W. Burby, L. Ellison, and Y. Zhou, *Nuclear Fusion* **56**, 014001 (2016).
- [85] Y. He, Y. Sun, H. Qin, and J. Liu, *Physics of Plasmas* **23**, 092108 (2016).
- [86] M. Kraus, K. Kormann, P. J. Morrison, and E. Sonnendrücker, *Journal of Plasma Physics* **83** (2017).
- [87] P. J. Morrison, *Physics of Plasmas* **24**, 055502 (2017).
- [88] J. Xiao, H. Qin, J. Liu, and R. Zhang, *Physics of Plasmas* **24**, 062112 (2017).
- [89] J. Xiao, H. Qin, and J. Liu, *Plasma Science and Technology* **20**, 110501 (2018).
- [90] J. Xiao, H. Qin, Y. Shi, J. Liu, and R. Zhang, *Physics Letters A* (2018), 10.1016/j.physleta.2018.12.010.
- [91] J. Xiao, H. Qin, P. J. Morrison, J. Liu, Z. Yu, R. Zhang, and Y. He, *Physics of Plasmas* **23**, 112107 (2016).
- [92] Y. Zhou, H. Qin, J. Burby, and A. Bhattacharjee, *Physics of Plasmas* **21**, 102109 (2014).

- [93] Y. Zhou, Y.-M. Huang, H. Qin, and A. Bhattacharjee, *Physical Review E* **93**, 023205 (2016).
- [94] Y. Zhou, *Variational Integration for Ideal Magnetohydrodynamics and Formation of Current Singularities*, Ph.D. thesis, Princeton University (2017).
- [95] Q. Chen, H. Qin, J. Liu, J. Xiao, R. Zhang, Y. He, and Y. Wang, *Journal of Computational Physics* **349**, 441 (2017).
- [96] Y. Shi, N. J. Fisch, and H. Qin, *Physical Review A* **94**, 012124 (2016).
- [97] Y. Shi, J. Xiao, H. Qin, and N. J. Fisch, *Physical Review E* **97**, 053206 (2018).
- [98] Y. Shi, *Plasma Physics in Strong Field Regimes*, Ph.D. thesis, Princeton University (2018).
- [99] H. Yoshida, *Physics Letters A* **150**, 262 (1990).
- [100] B. D. Fried and S. D. Conte, *The Plasma Dispersion Function* (Academic Press, 1968).
- [101] F. Romanelli, *Physics of Fluids B: Plasma Physics* **1**, 1018 (1989).
- [102] G. W. Hammett and F. W. Perkins, *Physical Review Letters* **64**, 3019 (1990).
- [103] S. C. Cowley, R. Kulsrud, and R. Sudan, *Physics of Fluids B: Plasma Physics* **3**, 2767 (1991).
- [104] W. Dorland and G. Hammett, *Physics of Fluids B: Plasma Physics* **5**, 812 (1993).
- [105] B. N. Rogers, W. Dorland, and M. Kotschenreuther, *Physical Review Letters* **85**, 5336 (2000).
- [106] A. Dimits, W. Nevins, D. Shumaker, G. Hammett, T. Dannert, F. Jenko, M. Pueschel, W. Dorland, S. Cowley, J. Leboeuf, T. Rhodes, J. Candy, and C. Estrada-Mila, *Nuclear Fusion* **47**, 817 (2007).
- [107] S. Ku, C. Chang, and P. Diamond, *Nuclear Fusion* **49**, 115021 (2009).
- [108] F. Merz and F. Jenko, *Nuclear Fusion* **50**, 054005 (2010).
- [109] J. Taylor, *Physical Review Letters* **6**, 262 (1961).
- [110] W. E. Drummond and M. N. Rosenbluth, *The Physics of Fluids* **5**, 1507 (1962).
- [111] R. Waltz, J. DeBoo, and M. Rosenbluth, *Physical Review Letters* **65**, 2390 (1990).
- [112] C. Petty, T. Luce, K. Burrell, S. Chiu, J. Degraessie, C. Forest, P. Gohil, C. Greenfield, R. Groebner, R. Harvey, *et al.*, *Physics of Plasmas* **2**, 2342 (1995).